Applied Physics Letters

Proximity-induced magnetism and the enhancement of damping in ferromagnetic/heavy metal systems

Cite as: Appl. Phys. Lett. **119**, 152401 (2021); https://doi.org/10.1063/5.0064336
Submitted: 22 July 2021 • Accepted: 29 September 2021 • Published Online: 11 October 2021

C. Swindells, H. Głowiński, Y. Choi, et al.

Applied Physics Letters ARTICLE scitation.org/journal/apl

Proximity-induced magnetism and the enhancement of damping in ferromagnetic/heavy metal systems

Cite as: Appl. Phys. Lett. **119**, 152401 (2021); doi: 10.1063/5.0064336
Submitted: 22 July 2021 · Accepted: 29 September 2021 ·
Published Online: 11 October 2021

C. Swindells,[1,2,a)] H. Głowiński,[3] Y. Choi,[4] D. Haskel,[4] P. P. Michałowski,[5] T. Hase,[6] P. Kuświk,[3] and D. Atkinson[1]

AFFILIATIONS

[1]Department of Physics, Durham University, South Road, Durham DH1 3LE, United Kingdom
[2]Department of Material Science and Engineering, University of Sheffield, Sheffield S1 3JD, United Kingdom
[3]Institute of Molecular Physics, Polish Academy of Sciences, Smoluchowskiego 17, 60-179 Poznań, Poland
[4]Advanced Photon Source, Argonne National Laboratory, Argonne, Illinois 60439, USA
[5]Łukasiewicz Research Network—Institute of Microelectronics and Photonics, Aleja Lotników 32/46, 02-668 Warsaw, Poland
[6]Department of Physics, University of Warwick, Coventry CV4 7AL, United Kingdom

[a)]**Author to whom correspondence should be addressed:** del.atkinson@durham.ac.uk

ABSTRACT

The relationship between proximity-induced magnetism (PIM) at the heavy metal/ferromagnet interface and spin-transport across such interfaces has generated significant debate. To investigate the link between the two, element specific x-ray magnetic circular dichroism and ferromagnetic resonance measurements were made on the same CoFe/Au/Pt and NiFe/Au/Pt thin film samples with varying Au thickness, with complementary SIMS analysis, which shows evidence of Ni diffusion from NiFe into the Pt. An approximately linear relationship is observed between the magnitude of Pt PIM and magnitude of damping enhancement in both systems. The results demonstrate that electronic hybridization of the heavy metal and ferromagnet is required for a full understanding of damping enhancement and interfacial spin-transport for spintronic devices.

A variety of phenomena at the interface between ferromagnetic (FM) and non-magnetic (NM) thin-film multilayered systems control nanomagnetic and spintronic behavior, the most significant being spin-dependent transport across the FM/NM interfaces, which underpins both giant[1,2] and tunnelling[3–7] magnetoresistance. When the NM layer is a heavy metal (HM), the propagation of pure spin-currents across the FM/HM interface yields fascinating behavior. For example, the injection of a spin-current from the HM into the FM, generated by the spin Hall effect,[8,9] produces a spin–orbit torque that can switch the FM magnetization. Alternatively, leakage of spin-current from the FM into the HM layer enhances the damping of ferromagnetic resonance via spin-pumping.[10–13] Electronic hybridization between the FM and HM layers can lead to a proximity-induced-magnetic moment (PIM) in the HM if it is close to the Stoner criterion,[14] which has been observed in Pt layered with transition metal ferromagnets using element specific x-ray magnetic circular dichroism (XMCD).[15–19] The influence and significance of PIM on spin transport across the interface between a HM and a magnetic layer have generated considerable research, particularly regarding the role of PIM in the enhancement of damping.[20–29] These studies report contradictory conclusions, either supporting or negating the role of PIM in spin transport and damping enhancement. For metallic FM/HM systems, a recent study, where Pt PIM was modified by alloying with Au, claimed irrelevance of PIM on interfacial spin torques.[22] Another concluded that spin memory loss was unaffected by PIM.[29] However, a ferromagnetic resonance (FMR) study reported that a reduction in Pt PIM resulted in a decrease in the interfacial contribution to damping.[20,30] The controversy is not limited to transition metal/HM systems, with studies of PIM and spin transport in ferrimagnetic YIG/Pt, reporting that PIM has either no effect, as determined from FMR measurements,[31] or a significant effect, from temperature-dependent spin Hall effect measurements[32] and angular-dependent FMR analysis.[33]

This paper reports a clear correlation between Pt PIM and damping in FM/Au/Pt systems, where Pt PIM is tuned by varying the Au

spacer layer. The magnitude of PIM is probed directly with Pt L-edge XMCD, and damping is measured with FMR. The correlation between PIM and damping is clearly established for two different FM layered systems. The unambiguous results not only show that PIM is critically relevant to the enhancement of the damping, but also indicate that spin pumping alone does not fully capture the physics behind interface enhanced damping, as is often assumed, and that electronic hybridization between the FM and HM polarized orbitals ought to be accounted for a complete understanding of spin transport in these systems.

Samples were grown using magnetron sputtering onto thermally oxidized Si substrates, with an Au spacer layer (SL) of increasing thickness along one dimension in both $Ni_{80}Fe_{20}$ (7 nm)/Au-wedge/Pt (4 nm) ($Ni_{80}Fe_{20}$ for simplicity, hereafter denoted as NiFe) and Cu (2 nm)/$Co_{25}Fe_{75}$ (7 nm)/Au-wedge/Pt (4 nm) systems ($Co_{25}Fe_{75}$, hereafter denoted as CoFe). The Au thickness was varied from 0 to 3 nm over a wedge distance of 16 mm. The thin-film CoFe alloy is expected to be bcc structured,[34] and the NiFe,[35] Au, and Pt to be fcc structured. Two additional samples capped with Cu but without the Pt layer were fabricated as reference structures. Critically, Au was selected as the spacer layer because although a ferromagnetic spin moment has been found in Au nanoparticles[36] and a Au PIM observed at the interface with Co[18] and NiFe,[37] the effect of an Au layer on the enhancement of damping is known to be small.[38] This is due to the large spin diffusion length of Au[39] and the filled 5*d* states,[40] so any induced moment on the Au will have a negligible impact on the interfacial spin transport phenomena.[41]

A schematic illustration of the wedge samples and the structural profiles of the two multilayered structures, determined from off resonance x-ray reflectivity (XRR), are shown in Fig. 1, at the thicker end of the Au wedge (2.2 nm), with a beam width of 0.1 mm. The XRR data were analyzed using the GenX code[42] to obtain best fitting scattering length density (SLD) profiles, which shows the uniform layer thicknesses and the interface transitions between the layers. Compositional sections were obtained using Secondary Ion Mass Spectrometry (SIMS) depth profiles, see also Fig. 1. The SIMS primary beam was rastered over $250 \times 250\ \mu m^2$, while the analysis area was limited to a rectangular region $10\,200\ \mu m^2$. Note the SIMS measurements reveal an extended Ni distribution beyond the NiFe layer toward the surface of the sample, which also corresponds with the different SLD observed in the Au region from the XRR analysis.

FMR measurements were made as a function of increasing Au thickness using a Vector Network Analyzer (VNA) and co-planar waveguide system over both wide frequency and magnetic field ranges at room temperature. Samples were placed face down on a waveguide and measured along the wedge at regular intervals. The 0.45 mm signal line excited a range of less than 0.1 nm of Au thicknesses. Figure 2(a) presents typical FMR data, with the insets showing examples of the real and imaginary components of the FMR signal at two frequencies and the main figure showing the magnetic field linewidth as a function of frequency, fitted with the linear relation,

$$\Delta H = \frac{4\pi\alpha}{\gamma} f + \Delta H_0, \tag{1}$$

where ΔH_0 is the extrinsic damping term, γ is the gyromagnetic ratio, and α is the Gilbert damping term, which contains both bulk and interfacial contributions.

For Cu-capped FM samples, the measured damping values of 0.0073 ± 0.0005 (NiFe) and 0.0055 ± 0.0003 (CoFe) are consistent

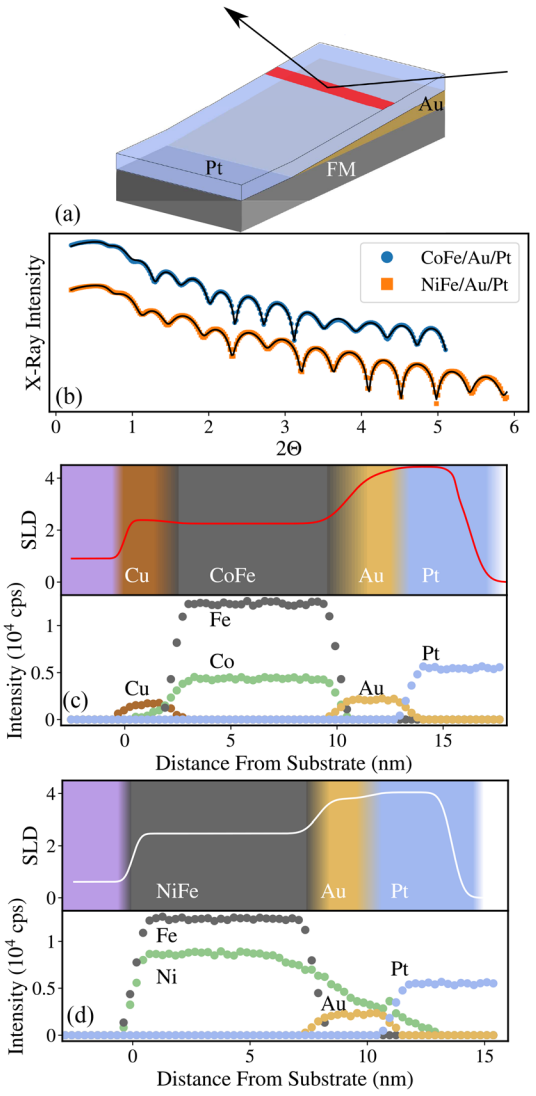

FIG. 1. (a) A schematic showing the thin film structure with an Au thickness wedge. The black arrow denotes the direction of beam propagation, with the red region representing the 0.1 mm area probed. (b) Examples of off resonance x-ray reflectivity data with best fits, taken at thicker Au spacer layer values with (c) and (d) corresponding scattering length density (SLD) profiles and element separated SIMS profiles for the two systems, showing the sample structures and interface widths.

with reported bulk damping values.[43,44] With an Au SL layer and a Cu cap, an increase in damping was observed with increasing Au thickness, with the enhancement above the bulk damping values being less than 10% for the CoFe and less than 20% for the NiFe case at the thickest Au SL. This difference in the magnitude of the damping enhancement may be associated with the crystal structure at the interface,[45] which is nominally fcc/fcc for NiFe/Au and bcc/fcc for CoFe/Au, and/or increased intermixing and Ni diffusion in the NiFe/Au system, which is evidenced from SIMS.

For the two FM/Au/Pt systems, the damping α is shown as a function of the Au spacer layer thickness in Fig. 2(b). Pt in direct

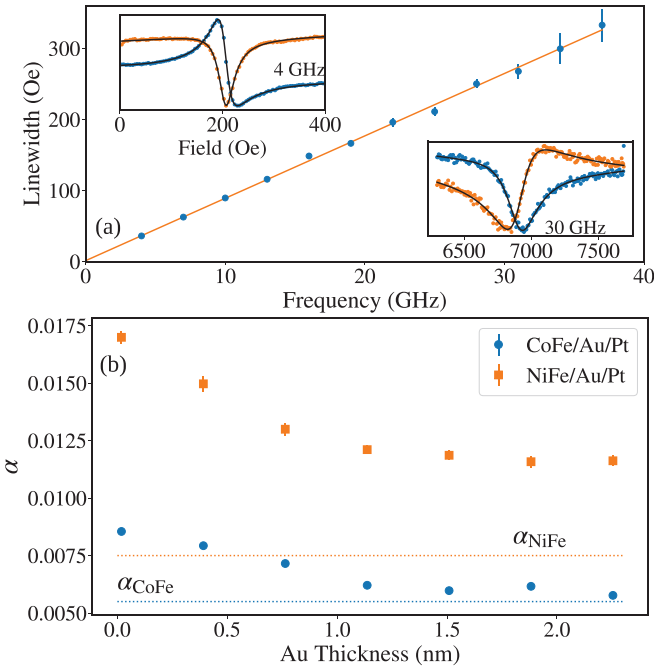

FIG. 2. (a) Representative frequency dependence of FMR field linewidth with the straight line fit for the NiFe/Au(0.7 nm)/Pt sample. Insets are examples of the real (blue) and imaginary (orange) data fitted as a function of field at 4 and 30 GHz, respectively. (b) The damping as a function of Au thickness for the Cu (2 nm)/CoFe (7 nm)/Au/Pt (4 nm) and NiFe (7 nm)/Au/Pt (4 nm) samples. The dotted lines indicate the bulk damping from the reference samples.

contact with the FM layer approximately doubles the damping compared with a Cu cap and 0 nm Au. For the CoFe/Au/Pt, the damping falls almost to the bulk value beyond 1.5 nm, the small remaining damping enhancement in the CoFe sample can be largely attributed to the Au interface mentioned earlier. In contrast, while the interfacial damping contribution initially falls in the NiFe/Au/Pt system with increasing Au thickness up to 1.5 nm, a significant enhancement in the damping persists for the thickest Au spacer. This persistent enhancement is much larger than the damping with an Au SL in the Cu capped reference sample, indicating a significant contribution from the Pt layer to the damping enhancement.

PIM in the Pt layer was probed in the same samples via Pt L3 edge (11.564 keV) XMCD measurements at the 4-ID-D beamline of the Advanced Photon Source, Argonne National Laboratory. The relative changes in the Pt PIM were measured in 2 mm steps along the Au SL wedge with a beam of width 25 μm. Element specific hysteresis loops and scans of the peak XMCD signal (a proxy for the moment) as a function of position along the wedge were both used to map the changes of Pt PIM with Au thickness. The measurements were made at a fixed angle of incidence of 2.28° with respect to the sample surface, with an energy dispersive fluorescence detector and a variable magnetic field of up to ±0.6 kOe applied in-plane and co-planar with the beam axis. At this angle, the x-ray beam penetrates the entire Pt and Au layers. The measured XMCD signal was taken as $\frac{I^+-I^-}{I^++I^-}$, where I^+ and I^- denote the spectra for opposite circular polarizations, for a fixed magnetic field.

The variations of the Pt PIM as a function of the Au SL thickness are shown in Fig. 3, an exponential fit was used to parameterize the PIM data for comparison with the damping data at the equivalent thicknesses. For both the CoFe and NiFe samples, the Pt XMCD signal falls exponentially over a similar length-scale (1.8 ± 0.2 nm) as the Au SL thickness increases. However, while the Pt PIM in the CoFe system effectively falls to zero beyond 1.5 nm of Au spacer, in contrast, in the NiFe sample, the Pt moment does not fall to zero, but to a sustained measurable value above 1.5 nm of Au. These trends are also evident in the hysteresis loops. The dependence of the Pt PIM on the Au SL thickness in these two systems gives the first indication of the relationship between Pt PIM and α, as shown in Fig. 2(b).

The persistence of a Pt PIM for all Au SL thicknesses in the NiFe sample is initially surprising but can be explained and allows for a direct comparison of Pt PIM and the enhancement of damping. While the two multilayered samples have the same nominal FM/Au/Pt structure, elemental mapping with SIMS reveals the distribution of Ni in the NiFe sample, which extends beyond the NiFe layer into the Au and Pt layers, see Fig. 1(d). The diffusion of Ni into the Pt enables $3d-5d$ hybridization beyond the immediate interface, which explains the Pt PIM measured for all Au SL thicknesses in the NiFe sample.

The relationship between the measured damping and the PIM in Pt is shown for both the CoFe and the NiFe samples in Fig. 4. This shows that a significant enhancement in the damping occurs only with

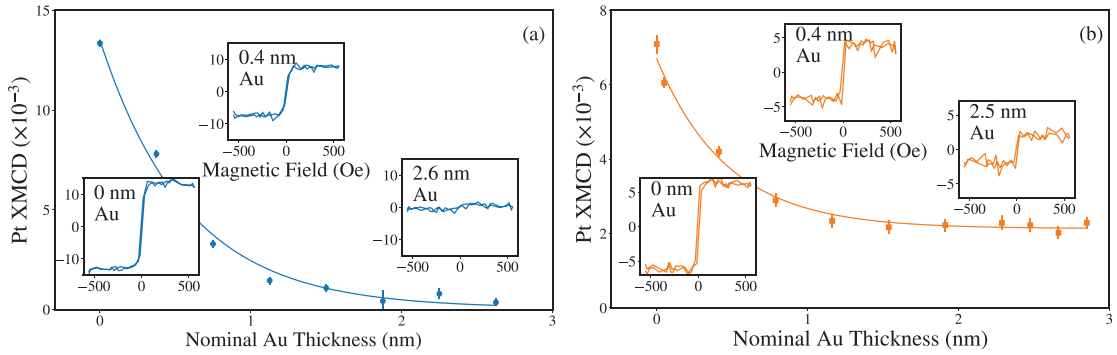

FIG. 3. Measured XMCD as a function of Au spacer thickness at both the Pt L_3 edge, with element specific hysteresis loops at three positions across the wedge inset, for (a) Cu (2 nm)/CoFe (7 nm)/Au/Pt (4 nm) and (b) NiFe (7 nm)/Au/Pt (4 nm). Solid lines are best fitting exponential functions.

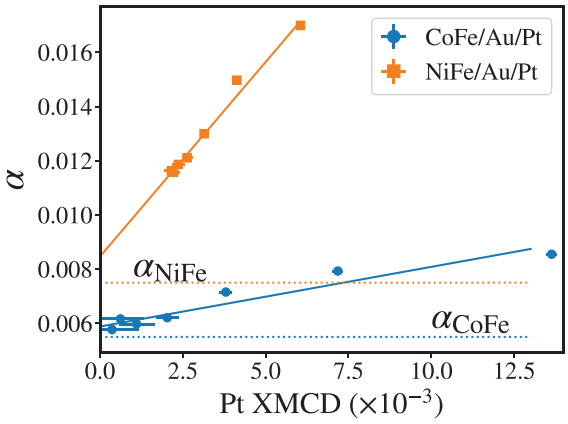

FIG. 4. Damping and Pt XMCD signals at the same points on the Au spacer wedge for the CoFe/Au/Pt and NiFe/Au/Pt samples. Note the dotted lines indicate the bulk damping contributions from the respective ferromagnetic layers.

a PIM in the Pt, and that the enhancement of the damping is directly proportional to the magnitude of the Pt PIM, irrespective of the interface quality or the presence of extended intermixing. Further details of the relationship between interface structure and PIM will be given in a subsequent paper.

The enhancement of the damping in FM/HM systems[46] is commonly explained within the spin pumping formalism, where non-equilibrium spin accumulation from increasingly damped processing magnetization in the FM drives a pure spin current across the interface into the HM.[11,47–49] This enhancement of the damping is determined by the efficiency of the spin transport across the interface, which depends upon the matching of spin conductance channels and the spin diffusion length of the HM.[10] In this formalism, PIM plays no role, as the equilibrium enhanced spin susceptibility does not affect the Sharvin conductance or the non-equilibrium transfer of spin current across the interface.[12] However, Omelchenko *et al.* explain that while PIM is not explicit in the mathematical representation of spin pumping, it plays an essential role in the quantitative values of key interfacial parameters, such as the spin mixing conductance. In particular, it was reported that the PIM acts to dephase the spin current, thereby shortening the spin diffusion length.[50] It has also been shown that a FM layer coupled to a magnetic layer near to T_c, rather than a NM layer, shows enhanced spin-pumping due to fluctuations of the interface spin conductance.[51,52]

An alternative explanation of interface-enhanced magnetization damping was developed by Barati *et al.*[53] using the tight-binding approach of Kambersky[54] that considers relaxation via inter- and intra-band transitions arising from spin–orbit coupling (SOC)[55] across the FM/HM interface. This theoretical approach showed that in contrast to Au that has little effect on the damping, layering with Pt and Pd significantly increases the damping, due to strong SOC and orbital hybridization with the 3d orbitals in the transition metal FM. Since this orbital hybridization is also responsible for PIM in the HM layer,[16] a clear connection between interfacial enhancement of damping and PIM emerges.

Though PIM is not the sole factor determining efficient spin transport across interfaces, these results highlight the relevance of PIM in interfacial spin transport and related spintronic phenomena, in marked contrast to conclusions of some previous reports.[22,29]

In conclusion, a direct relationship between the enhancement of damping and HM PIM was demonstrated, showing a significant enhancement of the damping occurs only with a PIM on the Pt, and the enhancement is directly proportional to the magnitude of the PIM. This relationship between PIM and the enhancement of damping opens questions about the physical basis for the enhanced damping, which suggest a reevaluation of the explicit role of PIM within the spin-pumping model and further theoretical consideration of the role of $3d-5d$ hybridization, which gives rise to PIM, in relation to the enhancement of the damping. More generally, these results indicate that PIM in HMs has wider implications in spintronics, such as for spin transport, that need further experimental investigation and theoretical consideration.

Funding is acknowledged from EPSRC for CS 1771248, Ref. EP/P510476/1 and the Royal Society for DA, IF170030. Support was acknowledged for beam time on 4-ID-D at the Advanced Photon Source supported by the U.S. Department of Energy, Office of Science, and Office of Basic Energy Sciences under Contract No. DE-AC02-06CH11357. Travel and subsistence were funded by the UK EPSRC XMaS facility. P.K. and H.G. acknowledge financial support from the National Science Centre Poland through the OPUS funding (Grant No. 2019/33/B/ST5/02013).

DATA AVAILABILITY

The data that support the findings of this study are openly available in Durham University website at http://doi.org/10.15128/r2qv33rw693, Ref. 56.

REFERENCES

[1]M. N. Baibich, J. M. Broto, A. Fert, F. N. Van Dau, F. Petroff, P. Etienne, G. Creuzet, A. Friederich, and J. Chazelas, "Giant magnetoresistance of (001) Fe/(001) Cr magnetic superlattices," Phys. Rev. Lett. **61**, 2472 (1988).
[2]G. Binasch, P. Grünberg, F. Saurenbach, and W. Zinn, "Enhanced magnetoresistance in layered magnetic structures with antiferromagnetic interlayer exchange," Phys. Rev. B **39**, 4828 (1989).
[3]M. Julliere, "Tunneling between ferromagnetic films," Phys. Lett. A **54**, 225–226 (1975).
[4]T. Miyazaki and N. Tezuka, "Giant magnetic tunneling effect in Fe/Al_2O_3/Fe junction," J. Magn. Magn. Mater **139**, L231–L234 (1995).
[5]J. S. Moodera, L. R. Kinder, T. M. Wong, and R. Meservey, "Large magnetoresistance at room temperature in ferromagnetic thin film tunnel junctions," Phys. Rev. Lett. **74**, 3273 (1995).
[6]J. Mathon and A. Umerski, "Theory of tunneling magnetoresistance of an epitaxial Fe/MgO/Fe (001) junction," Phys. Rev. B **63**, 220403 (2001).
[7]S. S. Parkin, C. Kaiser, A. Panchula, P. M. Rice, B. Hughes, M. Samant, and S.-H. Yang, "Giant tunnelling magnetoresistance at room temperature with MgO (100) tunnel barriers," Nat. Mater. **3**, 862–867 (2004).
[8]J. Hirsch, "Spin Hall effect," Phys. Rev. Lett. **83**, 1834 (1999).
[9]T. Kimura, Y. Otani, T. Sato, S. Takahashi, and S. Maekawa, "Room-temperature reversible spin Hall effect," Phys. Rev. Lett. **98**, 156601 (2007).
[10]Y. Tserkovnyak, A. Brataas, and G. E. Bauer, "Enhanced Gilbert damping in thin ferromagnetic films," Phys. Rev. Lett. **88**, 117601 (2002).
[11]A. Brataas, Y. Tserkovnyak, G. E. Bauer, and B. I. Halperin, "Spin battery operated by ferromagnetic resonance," Phys. Rev. B **66**, 060404 (2002).
[12]Y. Tserkovnyak, A. Brataas, G. E. Bauer, and B. I. Halperin, "Nonlocal magnetization dynamics in ferromagnetic heterostructures," Rev. Mod. Phys. **77**, 1375 (2005).

[13]C. Swindells, A. Hindmarch, A. Gallant, and D. Atkinson, "Spin transport across the interface in ferromagnetic/nonmagnetic systems," Phys. Rev. B **99**, 064406 (2019).
[14]E. C. Stoner, "LXXX. Atomic moments in ferromagnetic metals and alloys with non-ferromagnetic elements," Philos. Mag **15**, 1018–1034 (1933).
[15]J. Vogel, A. Fontaine, V. Cros, F. Petroff, J.-P. Kappler, G. Krill, A. Rogalev, and J. Goulon, "Structure and magnetism of Pd in Pd/Fe multilayers studied by x-ray magnetic circular dichroism at the Pd l 2, 3 sedges," Phys. Rev. B **55**, 3663 (1997).
[16]F. Wilhelm, P. Poulopoulos, G. Ceballos, H. Wende, K. Baberschke, P. Srivastava, D. Benea, H. Ebert, M. Angelakeris, N. Flevaris *et al.*, "Layer-resolved magnetic moments in Ni/Pt multilayers," Phys. Rev. Lett. **85**, 413 (2000).
[17]F. Wilhelm, P. Poulopoulos, H. Wende, A. Scherz, K. Baberschke, M. Angelakeris, N. Flevaris, and A. Rogalev, "Systematics of the induced magnetic moments in 5d layers and the violation of the third Hund's rule," Phys. Rev. Lett. **87**, 207202 (2001).
[18]F. Wilhelm, M. Angelakeris, N. Jaouen, P. Poulopoulos, E. T. Papaioannou, C. Mueller, P. Fumagalli, A. Rogalev, and N. Flevaris, "Magnetic moment of Au at Au/Co interfaces: A direct experimental determination," Phys. Rev. B **69**, 220404 (2004).
[19]R. Rowan-Robinson, A. Stashkevich, Y. Roussigné, M. Belmeguenai, S. Chérif, A. Thiaville, T. Hase, A. Hindmarch, and D. Atkinson, Sci. Rep. **7**, 16835 (2017).
[20]M. Caminale, A. Ghosh, S. Auffret, U. Ebels, K. Ollefs, F. Wilhelm, A. Rogalev, and W. Bailey, "Spin pumping damping and magnetic proximity effect in Pd and Pt spin-sink layers," Phys. Rev. B **94**, 014414 (2016).
[21]A. Conca, B. Heinz, M. Schweizer, S. Keller, E. Papaioannou, and B. Hillebrands, Phys. Rev. B **95**, 174426 (2017).
[22]L. Zhu, D. Ralph, and R. Buhrman, "Irrelevance of magnetic proximity effect to spin-orbit torques in heavy-metal/ferromagnet bilayers," Phys. Rev. B **98**, 134406 (2018).
[23]W. Amamou, I. V. Pinchuk, A. H. Trout, R. E. Williams, N. Antolin, A. Goad, D. J. O'Hara, A. S. Ahmed, W. Windl, D. W. McComb *et al.*, "Magnetic proximity effect in Pt/$CoFe_2O_4$ bilayers," Phys. Rev. Mater. **2**, 011401 (2018).
[24]M. Collet, R. Mattana, J.-B. Moussy, K. Ollefs, S. Collin, C. Deranlot, A. Anane, V. Cros, F. Petroff, F. Wilhelm *et al.*, "Investigating magnetic proximity effects at ferrite/Pt interfaces," Appl. Phys. Lett. **111**, 202401 (2017).
[25]X. Liang, G. Shi, L. Deng, F. Huang, J. Qin, T. Tang, C. Wang, B. Peng, C. Song, and L. Bi, "Magnetic proximity effect and anomalous hall effect in Pt/$Y_3Fe_{5-x}Al_xO_{12}$ heterostructures," Phys. Rev. Appl. **10**, 024051 (2018).
[26]M. Valvidares, N. Dix, M. Isasa, K. Ollefs, F. Wilhelm, A. Rogalev, F. Sánchez, E. Pellegrin, A. Bedoya-Pinto, P. Gargiani *et al.*, "Absence of magnetic proximity effects in magnetoresistive Pt/$CoFe_2O_4$ hybrid interfaces," Phys. Rev. B **93**, 214415 (2016).
[27]S. Geprägs, S. Meyer, S. Altmannshofer, M. Opel, F. Wilhelm, A. Rogalev, R. Gross, and S. T. Goennenwein, "Investigation of induced Pt magnetic polarization in Pt/$Y_3Fe_5O_{12}$ bilayers," Appl. Phys. Lett. **101**, 262407 (2012).
[28]S.-Y. Huang, X. Fan, D. Qu, Y. Chen, W. Wang, J. Wu, T. Chen, J. Xiao, and C. Chien, "Transport magnetic proximity effects in platinum," Phys. Rev. Lett. **109**, 107204 (2012).
[29]K. Gupta, R. J. Wesselink, R. Liu, Z. Yuan, and P. J. Kelly, "Disorder dependence of interface spin memory loss," Phys. Rev. Lett. **124**, 087702 (2020).
[30]M. Belmeguenai, M. Gabor, F. Zighem, N. Challab, T. Petrisor, R. Mos, and C. Tiusan, J. Phys. D: Appl. Phys. **51**, 045002 (2018).
[31]M. Weiler, M. Althammer, M. Schreier, J. Lotze, M. Pernpeintner, S. Meyer, H. Huebl, R. Gross, A. Kamra, J. Xiao, Y. Chen, H. Jiao, G. Bauer, and S. Goennenwein, Phys. Rev. Lett. **111**, 176601 (2013).
[32]Y. Lu, Y. Choi, C. Ortega, X. Cheng, J. Cai, S. Huang, L. Sun, and C. Chien, "Pt magnetic polarization on $Y_3Fe_5O_{12}$ and magnetotransport characteristics," Phys. Rev. Lett. **110**, 147207 (2013).
[33]S. Rezende, R. Rodríguez-Suárez, M. Soares, L. Vilela-Leão, D. Ley Domínguez, and A. Azevedo, "Enhanced spin pumping damping in yttrium iron garnet/Pt bilayers," Appl. Phys. Lett. **102**, 012402 (2013).
[34]M. A. Schoen, D. Thonig, M. L. Schneider, T. Silva, H. T. Nembach, O. Eriksson, O. Karis, and J. M. Shaw, "Ultra-low magnetic damping of a metallic ferromagnet," Nat. Phys. **12**, 839–842 (2016).
[35]M. A. W. Schoen, J. Lucassen, H. T. Nembach, T. J. Silva, B. Koopmans, C. H. Back, and J. M. Shaw, "Magnetic properties of ultrathin 3d transition-metal binary alloys. I. Spin and orbital moments, anisotropy, and confirmation of slater-Pauling behavior," Phys. Rev. B **95**, 134410 (2017).
[36]Y. Yamamoto, T. Miura, M. Suzuki, N. Kawamura, H. Miyagawa, T. Nakamura, K. Kobayashi, T. Teranishi, and H. Hori, "Direct observation of ferromagnetic spin polarization in gold nanoparticles," Phys. Rev. Lett. **93**, 116801 (2004).
[37]D. Burn, T. Hase, and D. Atkinson, "Focused-ion-beam induced interfacial intermixing of magnetic bilayers for nanoscale control of magnetic properties," J. Phys. Condens. Matter **26**, 236002 (2014).
[38]S. Azzawi, A. Ganguly, M. Tokac, R. Rowan-Robinson, J. Sinha, A. Hindmarch, A. Barman, and D. Atkinson, "Evolution of damping in ferromagnetic/nonmagnetic thin film bilayers as a function of nonmagnetic layer thickness," Phys. Rev. B **93**, 054402 (2016).
[39]M. Zeng, B. Chen, and S. T. Lim, "Interfacial electric field and spin-orbitronic properties of heavy-metal/CoFe bilayers," Appl. Phys. Lett. **114**, 012401 (2019).
[40]H. Wang, C. Du, Y. Pu, R. Adur, P. C. Hammel, and F. Yang, "Scaling of spin Hall angle in 3d, 4d, and 5d metals from $Y_3Fe_5O_{12}$/metal spin pumping," Phys. Rev. Lett. **112**, 197201 (2014).
[41]K. Shahbazi, A. Hrabec, S. Moretti, M. B. Ward, T. A. Moore, V. Jeudy, E. Martinez, and C. H. Marrows, "Magnetic properties and field-driven dynamics of chiral domain walls in epitaxial Pt/Co/Au_xPt_{1-x} trilayers," Phys. Rev. B **98**, 214413 (2018).
[42]M. Björck and G. Andersson, "Genx: An extensible x-ray reflectivity refinement program utilizing differential evolution," J. Appl. Crystallogr. **40**, 1174–1178 (2007).
[43]H. Głowiński, F. Lisiecki, P. Kuświk, J. Dubowik, and F. Stobiecki, "Influence of adjacent layers on the damping of magnetization precession in Co_xFe_{100-x} films," J. Alloys Compd. **785**, 891–896 (2019).
[44]M. A. W. Schoen, J. Lucassen, H. T. Nembach, B. Koopmans, T. J. Silva, C. H. Back, and J. M. Shaw, "Magnetic properties in ultrathin 3d transition-metal binary alloys. II. Experimental verification of quantitative theories of damping and spin pumping," Phys. Rev. B **95**, 134411 (2017).
[45]M. Tokac, S. Bunyaev, G. Kakazei, D. Schmool, D. Atkinson, and A. Hindmarch, "Interfacial structure dependent spin mixing conductance in cobalt thin films," Phys. Rev. Lett. **115**, 056601 (2015).
[46]S. Azzawi, A. Hindmarch, and D. Atkinson, "Magnetic damping phenomena in ferromagnetic thin-films and multilayers," J. Phys. D **50**, 473001 (2017).
[47]Y. Tserkovnyak, A. Brataas, and G. E. Bauer, "Spin pumping and magnetization dynamics in metallic multilayers," Phys. Rev. B **66**, 224403 (2002).
[48]A. Brataas, Y. Tserkovnyak, and G. E. Bauer, "Scattering theory of Gilbert damping," Phys. Rev. Lett. **101**, 037207 (2008).
[49]K. Ando, "Dynamical generation of spin currents," Semicond. Sci. Technol. **29**, 043002 (2014).
[50]P. Omelchenko, E. Girt, and B. Heinrich, "Test of spin pumping into proximity-polarized Pt by in-phase and out-of-phase pumping in Py/Pt/Py," Phys. Rev. B **100**, 144418 (2019).
[51]Y. Ohnuma, H. Adachi, E. Saitoh, and S. Maekawa, "Enhanced dc spin pumping into a fluctuating ferromagnet near t_c," Phys. Rev. B **89**, 174417 (2014).
[52]R. Bansal, N. Chowdhury, and P. Muduli, "Proximity effect induced enhanced spin pumping in Py/Gd at room temperature," Appl. Phys. Lett. **112**, 262403 (2018).
[53]E. Barati, M. Cinal, D. Edwards, and A. Umerski, "Gilbert damping in magnetic layered systems," Phys. Rev. B **90**, 014420 (2014).
[54]J. Kunes and V. Kamberskỳ, "First-principles investigation of the damping of fast magnetization precession in ferromagnetic 3d metals," Phys. Rev. B **65**, 212411 (2002).
[55]A. Sakuma, "First-principles study of the Gilbert damping constants of Heusler alloys based on the torque correlation model," J. Phys. D: Appl. Phys. **48**, 164011 (2015).
[56]C. R. Swindells (2021). "Proximity induced magnetism and the enhancement of damping in ferromagnetic/heavy metal systems [dataset]," Durham University, Dataset. https://doi.org/10.15128/r2qv33rw693